E-ISSN: 2717-3453 | P-ISSN: 2783-1442

Journal of Fuzzy Extension and Applications

www.journal-fea.com

J. Fuzzy. Ext. Appl. Vol. 2, No. 2 (2021) 171–190.

Paper Type: Research Paper

On the Prediction of COVID-19 Time Series: An Intuitionistic Fuzzy Logic Approach

Imo Eyo [1,*], Jeremiah Eyoh[2], Uduak Umoh[3]

[1] Department of Computer Science, University of Uyo, Uyo, Akwa Ibom State, Nigeria; imoheyoh@uniuyo.edu.ng;
[2] School of Electrical, Electronics and Systems Engineering, AVRRC, Loughborough University, Loughborough, UK; j.e.eyoh@lboro.ac.uk
[3] Department of Computer Science, University of Uyo, Uyo, Akwa Ibom State, Nigeria; j.e.eyoh@lboro.ac.uk.

Citation:

Eyo,I., Eyoh, J., & Umoh, U. (2021). On the prediction of COVID-19 time series: an intuitionistic fuzzy logic approach. *Journal of fuzzy extension and application*, 2(2), 171-190.

Received: 27/12/2020 Reviewed: 22/02/2021 Revised: 04/03/2021 Accepted: 27/03/2021

Abstract

This paper presents a time series analysis of a novel coronavirus, COVID-19, discovered in China in December 2019 using intuitionistic fuzzy logic system with neural network learning capability. Fuzzy logic systems are known to be universal approximation tools that can estimate a nonlinear function as closely as possible to the actual values. The main idea in this study is to use intuitionistic fuzzy logic system that enables hesitation and has membership and non-membership functions that are optimized to predict COVID-19 outbreak cases. Intuitionistic fuzzy logic systems are known to provide good results with improved prediction accuracy and are excellent tools for uncertainty modelling. The hesitation-enabled fuzzy logic system is evaluated using COVID-19 pandemic cases for Nigeria, being part of the COVID-19 data for African countries obtained from Kaggle data repository. The hesitation-enabled fuzzy logic model is compared with the classical fuzzy logic system and artificial neural network and shown to offer improved performance in terms of root mean squared error, mean absolute error and mean absolute percentage error. Intuitionistic fuzzy logic system however incurs a setback in terms of the high computing time compared to the classical fuzzy logic system.

Keywords: Pandemic; Coronavirus; Hesitation index; Gradient descent backpropagation algorithm.

1 | Introduction

The emergence of COVID-19 (coronavirus disease 2019) in December, 2019 has shaken and brought the whole world for some weeks/months of lockdown due to extreme loss of lives [1]. COVID-19 is a severe acute respiratory syndrome coronavirus 2 (SARS-CoV-2) [2]. SARS-CoV-2 is highly contagious and has presented a major global health threat [3]. Reports from the World Health Organization (WHO) indicate that the world records 10,357,662 confirmed cases of COVID-19 with 508,055 deaths until July 1st, 2020, 6:08 pm CEST [1]. It is therefore incumbent

Corresponding Author: imoheyoh@uniuyo.edu.ng
http://dx.doi.org/10.22105/jfea.2021.263890.1070

on the Governments, private organizations and individuals to take necessary steps to combat this global pandemic.

COVID-19 is known to emanate from Wuhan, China with rapid spread to surrounding countries such as Korea, Thailand and Japan, and from there to Europe, America, and later to Africa [4]. The most affected countries in Africa are South Africa, Egypt, Nigeria and Ghana respectively. Here, the focus is on Nigeria, the most populous country in Africa with population of over 200 million people, which contributes to about 2.64% of the world population. The Nigeria Center for Disease Control (NCDC) recorded the first case of coronavirus in Nigeria on February 28th, 2020 and the first death on March 23rd, 2020. Currently, Nigeria is experiencing a steady but exponential growth in the confirmed cases of COVID-19 across the country. As reported on July 1st, 2020, 6:08 pm CEST, the number of confirmed cases of COVID-19 in Nigeria have risen to 25,694 with 590 deaths, making Nigeria the third most affected country in Africa.

To curb the propagation of COVID-19, cities in Nigeria and other African countries have been locked down for weeks until recently, with a gradual easing of the lockdown. In Nigeria, the NCDC provided strict preventive measures, such as washing of hands thoroughly and frequently with soap under running water, quarantining symptomatic persons and isolating infected persons, promoting social distancing and wearing of facemask especially in public places for self-protection. Other ways to curtail the spread of COVID-19 included restrictions on public gathering, travelling (banned interstate travelling) except for essential workers, closing of schools, and offices. Exclusions were however granted to grocery stores, pharmacies, public markets, and other stores selling food and essential products. There was a complete lockdown in major cities like Abuja - the Federal Capital Territory, Lagos and Ogun states and later in all the states of the federation. Despite these preventive efforts, the COVID-19 cases in Nigeria are gradually increasing and steps must be taken to accurately predict the COVID-19 pandemic. In this study, the use of intuitionistic fuzzy set to predict COVID-19 pandemic cases in Nigeria is proposed. The objective of this study is to ascertain the performance of hesitation-enabled intuitionistic fuzzy set on the prediction of COVD-19 pandemic and to compare its performance with the traditional fuzzy set and artificial neural network. To the best knowledge of the authors, this is the first study that predict COVID-19 pandemic cases using intuitionistic fuzzy logic system that utilizes intuitionistic fuzzy sets with optimized parameters.

The rest of the paper is organized as follows: Section 2 has the literature review while Section 3 discusses the methodology adopted to solve the COVID-19 prediction problem. Performance evaluation is presented in Section 4 while conclusion is drawn in Section 5.

2 | Literature Review

Many studies have been conducted for the prediction of COVID-19 pandemic all over the world. For instance, Bastos and Cajueiro [5] forecasted the early evolution of COVID-19 in Brazil using two modified versions of the Susceptible-Infected Recovered (SIR) epidemic model. The data for the forecast was collected from February 25th, 2020 to March 30th, 2020 and the results from their short-term forecast were in tandem with the collected data. In the same vein, Pandey et al. [3] proposed the use of Susceptible, Exposed, Infectious, recovered (SEIR) and regression models to predict the COVID-19 confirmed cases in India. The two models were found to effectively analyze and predict COVID-19 disease in India.
However, according to [6], COVID-19 has some characteristic features that are quite distinct from other existing infectious diseases. These features make it difficult to apply SIR and SEIR models directly to COVID-19 data. Therefore, Zhao and Chen [6] proposed the Susceptible, Un-quarantined infected, quarantined infected, Confirmed infected (SUQC) model. The authors noted that the SUQC is able to characterize the dynamics of COVID-19 and provided accurate prediction on the test data better than other epidemic models. Patra et al. [2] presented long short-term memory (LSTM) networks for the prediction of COVID-19 data in India, USA, Argentina and Brazil. The authors adopted 90% of

Eyo et al. | J. Fuzzy. Ext. Appl. 2(2) (2021) 171-190

the data for the countries under study as training data while 10% was used as test data. The results of LSTM were compared with convolutionary neural network and nonlinear autoregressive time series and found to outperform both in terms of the nine-error metrics adopted for the study. Roosa et al. [7] proposed a COVID-19 epidemic forecast in China that operates in real time from February 5th to February 24th, 2020 using the sub-epidemic model. Their proposed sub-epidemic model was compared with generalized logistic growth model and Richards**'s** model and found to provide a good forecast in terms of the mean squared error. Anastassopoulou et al. [8] adopted the Susceptible-Infectious-Recovered-Dead (SIRD) epidemic model in the prediction of COVID-19 outbreak in Hubei, China. The data was collected from a publicly available database from January 11th to February 10th, 2020 and analysis of results show that the evolution of the COVID-19 pandemic was within the bounds of the forecast.

As a global pandemic, prediction of COVID-19 outbreak has been conducted for several other countries including Canada [9], Saudi Arabia [10], Italy, Spain and France [11], Brazil [5] and [12], Hungary [13], Italy [14] and [15] Malaysia [16], Japan [17], Iran [18] and more. Petropoulos and Makridakis [19] presented a statistical forecast of COVID-19 confirmed cases using robust time series. The COVID-19 data collected consisted of cumulative daily figures aggregated globally and captured three cases namely: confirmed cases, deaths and recoveries. The data was obtained from John Hopkins University of daily cumulative cases from January 22, 2020 to March 11, 2020. Simple time series from the family of exponential smoothing was adopted and shown to produce good forecast. According to [8], the official data provided for COVID-19 is highly uncertain and according to [20], fuzzy logic is a concept that connotes uncertainty and can adequately model the same. This calls for the utilization of fuzzy logic tools that can adequately cope with uncertainty in the COVID-19 data. To achieve this, many researchers have adopted and integrated fuzzy logic in the prediction models. For instance, Patra et al. [2] has proposed the use of multiple ensemble neural network models with fuzzy response aggregation for the prediction of the COVID-19 time series in Mexico. The main essence of the integration of fuzzy response aggregation was to manage the uncertainty occasioned by the individual networks, thus leading to lower uncertainty. The proposed approach was shown to provide good estimation when compared with the actual values and other prediction models. Al-Qaness et al. [21] proposed the use of adaptive neuro-fuzzy inference system (ANFIS) optimized with flower pollination algorithm (FPA) and salp swarm algorithm (SSA) to estimate and forecast the confirmed cases of COVID-19 in China. According to the authors, the performance of FPASSA-ANFIS in terms of the predicted values of the confirmed COVID-19 is very high and outperforms other models in terms of RMSE, MAE, MAPE, root mean squared relative error (RMSRE), coefficient of determination (R2) and computing time. Other studies such as Dhiman and Sharma [22] proposed a fuzzy logic inference for identification and prevention of COVID-19. Fong et al. [23] proposed the use of hybridized deep learning and fuzzy rule induction for the analysis of COVID-19 outbreak. Fatima et al. [24] presented Internet of Things (IoT) which enabled smart monitoring of COVID-19 with associated fuzzy inference system. Verma et al. [25] applied arima and fuzzy time series models while Van Tinh [26] utilized fuzzy time series model in combination with particle swarm optimization for COVID-19 prediction.

All the previous works make use of classical type-1 fuzzy logic systems (FLSs) for the prediction of COVID-19 outbreak with the aim of modelling uncertainty in the data. The classical FLS can only handle uncertainty by defining membership functions with the assumption that every non-membership function is complementary to the membership function. This assumption may not always be correct, as there may be some hesitations surrounding membership and non-membership functions of an element to a set. Kumar [27] put it clearly that the hesitation occurring in the membership degrees cannot be integrated in a fuzzy set theory.

To this end, the use of intuitionistic fuzzy set (IFS) introduced in 1999 by Atanassov [28] for the prediction of COVID-19 pandemic cases in Nigeria is proposed in this study. An IFS is a fuzzy set format that is defined using both Membership Functions (MFs) and Non-Membership Functions (NMFs), which are independent from each other, with extra parameter known as the hesitation degree (index).

Literature is replete with studies involving IFS such as prediction and time series forecasting [20,] [29], [30], [31], [32], [33], [34], and [35], multi-criteria decision making [36], control [37], temporal fault trees analysis [38], system failure probability analysis [39], data envelopment analysis [40], estimating correlation coefficient between IFSs with hesitation index [41] and more. The motivation behind this study is that by using IFLS to analyze COVID-19 pandemic data, more information will be captured and uncertainty efficiently handled. Moreover, the IFSs enable hesitation which is preponderant in humanlanguage representation, thus providing more adequate and concordant solutions to the real-world (COVID-19) problem than its classical counterpart in terms of providing better advantages in handling vagueness and uncertainty. For instance, Khatibi and Montazer [42] adopted the classical FS and IFS in medical diagnosis for the detection of intestinal bacteria that causes typhoid fever and dysentery by using different similarity measures of FS and IFS. According to the authors, although both Fs and IFS are strong tools for uncertainty modeling, analyses in Khatibi and Montazer [42] show that IFS provided more accurate results than the classical FS. According to [39], the IFS, defined with separate membership and non-membership degrees has much wider range of applicability than traditional fuzzy set theory. In otherwords, as Rahman et al. [43] state, IFS stands as an important tool in managing with imprecision.

Themaincontribution of this paper, therefore is the adoption of parameter optimized intuitionistic fuzzy logicsystem (IFLS) which captures some level of hesitation in the MFs and NMFs. The inclusion of the intuitionistic fuzzy index in the COVID-19 pandemic prediction provides flexibility and tends to agree with human reasoning and information representation better. The integration of hesitation index component in the modelling of uncertainty in COVID-19 data is an interesting direction followed in this analysis. To aid comparison, the traditional type-1 fuzzy logic system is also constructed and evaluated using the COVID-19 pandemic cases.

3 | Methodology

In this section, the traditional type-1 FS is briefly discussed. The IFS, IFLS and parameter update for IFLS MF and NMF are derived. The datasets used for evaluating the proposed model are also described.

3.1 | Fuzzy Sets (Classical Fuzzy Set and Intuitionistic Fuzzy Set)

The classical FS introduced by Zadeth [44] is an extended version of the traditional binary set. Unlike binary set with 0 or 1 membership value, FS membership falls in a closed interval [0, 1].

Definition 1. A classical FS is characterised by only the MF, $\mu_A(x)$ which specifies the degree of belonging of an element to a set, i.e., $A = \{(x, \mu_A(x)) | \forall x \in X\}$.

Any system that adopts one or more type-1 FS is known as type-1 FLS. This assumption may not be applied to every situation as they may be some hesitation from the expert in determining the degree of membership of an element to a set. This extra parameter may not simply be classified as MF or NMF. This calls for another kind of FS known as the IFS which provides some flexibility in terms of the hesitation degree. Thus, the IFS is an extended version of the traditional type-1 FS.

Definition 2. [28]. An IFS is defined by both MF, $\mu_{A^*}(x) \in [0,1]$ and NMF, $\nu_{A^*}(x) \in [0,1]$ such that $0 \leq \mu_{A^*}(x) + \nu_{A^*}(x) \leq 1$.

Eyo et al. | J. Fuzzy. Ext. Appl. 2(2) (2021) 171-190

An IFS has an additional parameter called the hesitation index, $\pi(x)$ such that $\pi_{A^*}(x)=1-(\mu_{A^*}(x)+\nu_{A^*}(x))$. Obviously, when $(\mu_{A^*}(x)+\nu_{A^*}(x))=1$, a traditional type-1 FS is obtained. Radhika and Parvathi [45], Hájek and Olej [46] and Mahapatra and Roy [47] have formulated ways of defining the MF and NMF of an IFS. In this work, the MF and NMF (see *Fig. 1*) are defined following the approach in [45] using Gaussian

$$\mu_{ik}(x_i)=\exp\left(-\frac{(x_i-c_{ik})^2}{2\sigma^2}\right)-\pi, \tag{1}$$

$$\nu_{ik}(x_i)=1-\exp\left(-\frac{(x_i-c_{ik})^2}{2\sigma^2}\right), \tag{2}$$

function as follows:

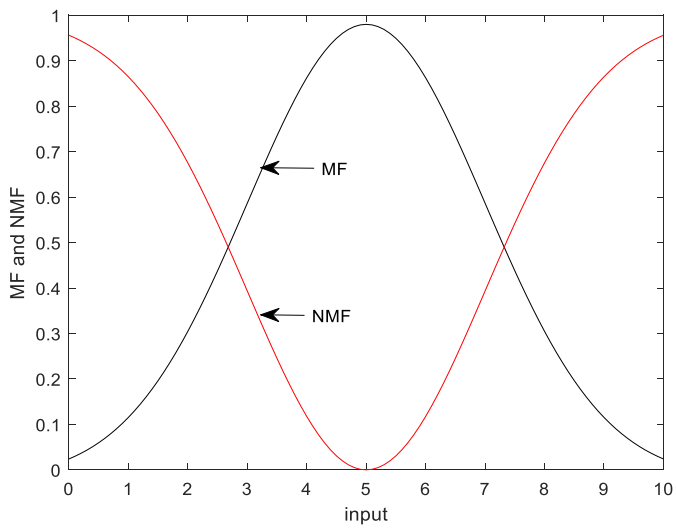

Fig. 1. Intuitionistic fuzzy set [48].

where $\mu(x)$ is the MF and $\nu(x)$ is the NMF, x is the input, σ and c are the standard deviation and center of the IFS respectively while $\pi\in[0,1]$ is the hesitation index, otherwise known as intuitionistic fuzzy index. For all the experiments, the hesitation index was chosen as 0.1. A system that uses IFS in either its antecedent and/or consequent part(s) is known as IFLS.

3.2 | Intuitionistic Fuzzy Logic System

An IFLS (see *Fig. 2*) possesses the same functionalities as the traditional FLS namely: the fuzzifier, rule based, inference engine and defuzzifier. The only exception is that the different parts are intuitionistic based (with hesitation indices).

3.2.1 | Fuzzification

Similar to the classical FS, fuzzification involves converting crisp inputs into MFs and NMFs which are fed into the intuitionistic inference engine and translated into intuitionistic fuzzy output set. Here, singleton fuzzification is assumed. That is, $\mu_{A^*}(x)=\begin{cases}1/1 & if\ x=x'\\ 1/0 & if\ x\neq x'\end{cases}$.

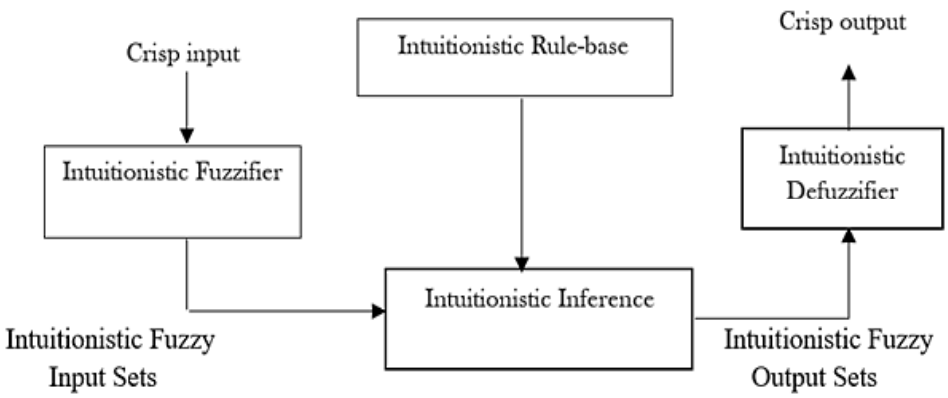

Fig. 2. Intuitionistic fuzzy logic system [48].

3.2.2 | Rules

The generic rule structure of IFLSs is as below

$$R_k : \text{if } x_i \text{ is } A^*_{ik} \text{ and ... and } x_n \text{ is } A^*_{nk} \text{ then } y_k = \sum_{i=1}^{n} w_{ik} x_i + b_k . \quad (3)$$

Which can be reformulated for MF and NMF as follows:

$$R^{\mu}_k : \text{if } x_i \text{ is } A^{*\mu}_{ik} \text{ and ... and } x_n \text{ is } A^{*\mu}_{nk} \text{ then } y^{\mu}_k = \sum_{i=1}^{n} w^{\mu}_{ik} x_i + b^{\mu}_k , \quad (4)$$

$$R^{\nu}_k : \text{if } x_i \text{ is } A^{*\nu}_{ik} \text{ and ... and } x_n \text{ is } A^{*\nu}_{nk} \text{ then } y^{\nu}_k = \sum_{i=1}^{n} w^{\nu}_{ik} x_i + b^{\nu}_k . \quad (5)$$

Where x's represent the inputs, y_k's are rule's outputs, A^*'s are IFSs, w represents the weight and b, the bias. Once the intuitionistic fuzzy rules are established, the IFLS can be seen as a mapping from inputs to outputs with the mapping quantitatively represented as $y = f(x)$.

3.2.3 | Inference

This study adopts a Takagi-Sugeno-Kang (TSK) inference. Here the IF-THEN rules in the rule base are combined into a mapping from an input linguistic vector to an output variable, y. For TSK inference, the output is a linear combination of the inputs.

Eyo et al. | J. Fuzzy. Ext. Appl. 2(2) (2021) 171-190

3.2.4 | Defuzzification

In order to obtain a crisp value for the output of a FLS, the defuzzification procedure is often employed. This work adopts the defuzzification method proposed in [49] where the outputs of each subsystems (MF and NMF) are computed and then combined to produce the final output. Hájek and Olej [49] defined the final output of a TSK-type IFLS as follows:

$$y = (1-\beta)\sum_{k=1}^{M} \tilde{f}^{\mu} y_k^{\mu} + \beta \sum_{k=1}^{M} \tilde{f}^{\nu} y_k^{\nu} . \tag{6}$$

Where:

$$\tilde{f}^{\mu} = \frac{f_k^{\mu}}{\sum_{k=1}^{M} f_k^{\mu}} , \tag{7}$$

and

$$\tilde{f}^{\nu} = \frac{f_k^{\nu}}{\sum_{k=1}^{M} f_k^{\nu}} . \tag{8}$$

And $\tilde{f}^{\mu}$ and $\tilde{f}^{\nu}$ are normalized firing magnitude for MFs and NMFs respectively while β is the user defined parameter which controls how much MF and NMF support the final output. The MF alone contributes to the final output if β is 0 and NMF alone contributes to the final output if β is 1. However, when $0 \le \beta \le 1$, the output is formed by both MFs and NMFs.

3.3 | Parameter Update

The problem under investigation is an optimization problem and requires adjustment of the parameters of the MF and NMF of the IFLS. The popular Gradient Descent (GD) back propagation algorithm is used to optimize these parameters. The cost function for a single output is defined as

$$E = \frac{1}{2}\left(y^{a} - y\right)^{2} . \tag{9}$$

Where y^a is the actual output and y is the predicted output. The parameters of IFLS to be updated include the center, c, standard deviation, σ, weight, w, bias, b and β.

For GD optimization, any generic parameter, θ, can be updated as follows

$$\theta_{ik}(t+1) = \theta_{ik}(t) - \gamma \frac{\delta E}{\delta \theta_{ik}} . \tag{10}$$

Where γ is the learning rate that controls the learning process and must be chosen carefully to avoid instability or slow learning. The parameters of the consequent parts include the weights (w) and biases (b) and updated as follows:

$$w_{ik}(t+1) = w_{ik}(t) - \gamma \frac{\delta E}{\delta w_{ik}}, \tag{11}$$

and

$$b_{ik}(t+1) = b_{ik}(t) - \gamma \frac{\delta E}{\delta b_{ik}}. \tag{12}$$

Respectively, the derivative with respect to the weight is computed as in *Eq. (13)* and *Eq. (14)*.

$$\frac{\delta E}{\delta w_{ik}} = \frac{\delta E}{\delta y}\frac{\delta y}{\delta y_k}\frac{\delta y_k}{\delta w_{ik}} = \sum_{k=1}^{M} \frac{\delta E}{\delta y}\left[\frac{\delta y}{\delta y_k^{\mu}}\frac{\delta y_k^{\mu}}{\delta w_{ik}^{\mu}} + \frac{\delta y}{\delta y_k^{\nu}}\frac{\delta y_k^{\nu}}{\delta w_{ik}^{\nu}}\right]. \tag{13}$$

$$\left(y(t) - y^{a}(t)\right)\left[(1-\beta)\left(\frac{f_k^{\mu}}{\sum_{k=1}^{M} f_k}\right) + \beta\left(\frac{f_k^{\nu}}{\sum_{k=1}^{M} f_k}\right)\right] x_i. \tag{14}$$

While the derivative with respect to the bias is as in *Eq. (15)* and *Eq. (16)* respectively.

$$\frac{\delta E}{\delta b_{ik}} = \frac{\delta E}{\delta y}\frac{\delta y}{\delta y_k}\frac{\delta y_k}{\delta b_{ik}} = \sum_{k=1}^{M} \frac{\delta E}{\delta y}\left[\frac{\delta y}{\delta y_k^{\mu}}\frac{\delta y_k^{\mu}}{\delta b_{ik}^{\mu}} + \frac{\delta y}{\delta y_k^{\nu}}\frac{\delta y_k^{\nu}}{\delta b_{ik}^{\nu}}\right], \tag{15}$$

$$\left(y(t) - y^{a}(t)\right)\left[(1-\beta)\left(\frac{f_k^{\mu}}{\sum_{k=1}^{M} f_k}\right) + \beta\left(\frac{f_k^{\nu}}{\sum_{k=1}^{M} f_k}\right)\right] x_i. \tag{16}$$

The Gaussian function is adopted to construct the MF.

$$\mu_{ik}(x_i) = \exp\left(-\frac{(x_i - c_{ik})^2}{2\sigma^2}\right). \tag{17}$$

The Gaussian function in *Eq. (17)* is modified as in *Eq. (18)* and *Eq. (19)* to reflect membership and non-membership functions of IFS respectively.

$$\mu_{ik}(x_i) = \exp\left(-\frac{(x_i - c_{ik})^2}{2\sigma^2}\right) - \pi, \tag{18}$$

$$\nu_{ik}(x_i) = 1 - \exp\left(-\frac{(x_i - c_{ik})^2}{2\sigma^2}\right). \tag{19}$$

Where π is the intuitionistic fuzzy index defining the hesitation of the expert in specifying MFs and NMFs. The antecedent parameters are the center (c) and standard deviation (σ) which are updated as in *Eq. (20)* and *Eq. (21)* respectively.

Eyo et al.|J. Fuzzy. Ext. Appl. 2(2) (2021) 171-190

$$c_{ik}(t+1) = c_{ik}(t) - \gamma \frac{\delta E}{\delta c_{ik}}, \tag{20}$$

and

$$\sigma_{ik}(t+1) = \sigma_{ik}(t) - \gamma \frac{\delta E}{\delta \sigma_{ik}}. \tag{21}$$

Where the derivative $\frac{\delta E}{\delta c_{ik}}$ in *Eq. (20)* is calculated as follows:

$$\frac{\delta E}{\delta c_{ik}} = \sum_{k=1}^{M} \frac{\delta E}{\delta y}\left[\frac{\delta y}{\delta f_k^{\mu}}\frac{\delta f_k^{\mu}}{\delta \mu_{ik}}\frac{\delta \mu_{ik}}{\delta c_{ik}} + \frac{\delta y}{\delta f_k^{\nu}}\frac{\delta f_k^{\nu}}{\delta \nu_{ik}}\frac{\delta \nu_{ik}}{\delta c_{ik}}\right], \tag{22}$$

and the derivative in *Eq.(21)* is computed as follows:

$$\frac{\delta E}{\delta \sigma_{ik}} = \sum_{k=1}^{M} \frac{\delta E}{\delta y}\left[\frac{\delta y}{\delta f_k^{\mu}}\frac{\delta f_k^{\mu}}{\delta \mu_{ik}}\frac{\delta \mu_{ik}}{\delta \sigma_{ik}} + \frac{\delta y}{\delta f_k^{\nu}}\frac{\delta f_k^{\nu}}{\delta \nu_{ik}}\frac{\delta \nu_{ik}}{\delta \sigma_{ik}}\right]. \tag{23}$$

The parameters of the classical type-1 FS are also updated the same way using the generic GD backpropagation algorithm in *Eq. (10)*. However, for classical FS, only the MF parameters are optimized. Shown in Algorithm 1 is the complete procedure for GD learning of the parameters of IFLS. The same procedure applies to classical type-1 FLS. The IFLS-GD was implemented in MATLAB® 2020.

Algorithm 1: IFLS-GD Learning Procedure

INPUT: training set, centre (c), standard deviation (σ), weight (w), bias (b), hesitation index (π), user defined parameter (β), learning rate (γ)

(1) Set initial training epoch to 1
(2) Set training data to 1
(3) Propagate the training data through the IFLS model.
(4) Using Eq. (11) and (12), tune the consequent parameters of IFLS.
(5) Calculate the output of IFLS using Eq. (6)
(6) Calculate the difference between the actual output and predicted output of IFLS with root mean squared error (RMSE) as the cost function.
(7) Backpropagate the error and tune the antecedent parameters using Eq. (20) and (21).
(8) Increment the training data by 1. If training data ≤ total number of training samples, go to step 3 else increment training epoch by 1
(9) If maximum epoch is reached END; else,
(10) Go to step 3.

OUTPUT: Prediction error

3.4 | Dataset Description

The Nigeria COVID-19 pandemic cases used in this study are extracted from Kaggle, a publicly available data repository [50] which houses COVID-19 data for all African countries. The dataset was captured from February 15th (as other African countries had confirmed cases from this day, however, the first case in Nigeria was reported on February 28th, 2020) to June 24th, 2020. The dataset contains 5 cases of COVID-19 outbreak in Nigeria namely: daily cases, daily deaths, active cases, total cases and total deaths. In this study, prediction is done for each COVID-19 case in Nigeria using present and past values to predict a one-step future value. According to [51], prediction can be qualitative, explanatory or time series in nature. In this study, each of the COVID-19 case dataset is modelled as time series which involves sequential collections of data over time [20]. The task here is a short-term forecast where a day-ahead prediction is carried out. The time series is represented as:

$$Y(t+1)=f\left[x(t),x(t-1),...,x(t-s+1)\right], \tag{24}$$

Where f is a function representing the model of prediction and s is the input size. For four inputs adopted in this study, the current input and three previous inputs of the time series are utilized giving the input generating vector as $\left[x(t);x(t-1);x(t-2);x(t-3)\right]$ while $Y(t+1)$ represents the output. Whilst the current value of the time series helps to keep an up-to-date measurement of COVID-19 case, the previous values keep track of the trend. Before the analysis, the collected COVID-19 cases data are normalized to a small range between 0 and 1 using the min-max normalization as follows:

$$x_{new}=\frac{x_i-\min(X)}{\max(X)-\min(X)}. \tag{25}$$

Where x is the data instant of input variable, X, $min(X)$ and $max(X)$ represent the minimum and maximum values of variable, X. To obtain the actual predicted (non-normalized) values, the normalized predicted outputs are converted back to the original scale using *Eq. (26)*.

$$Xnew=IFLS_{predictedOutput}*(\max(trainingData)-\min(trainingData))+\min(trainingData). \tag{26}$$

Shown in *Fig. 3* is the structure of IFLS with two inputs and three MFs and NMFs.

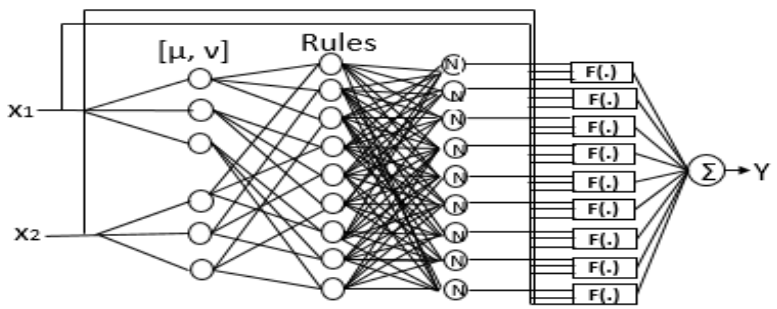

Fig. 3. Architecture of IFLS [48].

The time series are split into 70% training and 30% testing instances respectively. For an objective evaluation of the cases, the experiments are conducted 10 times and the average results are computed.

Eyo et al. | J. Fuzzy. Ext. Appl. 2(2) (2021) 171-190

The epoch was kept at 100 and the learning rate chosen as 0.1. The normalized training data are then propagated into the IFLS as shown in *Fig. 3*. As shown in *Fig. 3*, the inputs are first passed forward into the fuzzifier to obtain the MF (μ) and NMF (ν) of IFLS, the rules are generated, and depending on the firing strength, the outputs are obtained. *Table 1* is a snapshot of the different COVID-19 cases from the first day (28th February) of confirmed case in Nigeria up to March 31st, 2020. *Fig. 4* shows the trend of the COVID-19 outbreak in Nigeria for the period of February 15th, 2020 to June 24th, 2020.

Table 1. Snapshot of COVID-19 cases in Nigeria from 28th February to 31st March, 2020.

Date	Daily cases	Daily Deaths	Active Cases	Total Cases	Total Deaths
Feb-28	1	0	1	1	0
Feb-29	0	0	1	1	0
Mar-01	0	0	1	1	0
Mar-02	0	0	1	1	0
Mar-03	0	0	1	1	0
Mar-04	0	0	1	1	0
Mar-05	0	0	1	1	0
Mar-06	0	0	1	1	0
Mar-07	0	0	1	1	0
Mar-08	0	0	1	1	0
Mar-09	1	0	2	2	0
Mar-10	0	0	2	2	0
Mar-11	0	0	2	2	0
Mar-12	0	0	2	2	0
Mar-13	0	0	2	2	0
Mar-14	0	0	2	2	0
Mar-15	0	0	1	2	0
Mar-16	0	0	1	2	0
Mar-17	1	0	2	3	0
Mar-18	5	0	7	8	0
Mar-19	4	0	11	12	0
Mar-20	0	0	11	12	0
Mar-21	10	0	21	22	0
Mar-22	8	0	28	30	0
Mar-23	10	1	37	40	1
Mar-24	4	0	41	44	1
Mar-25	7	0	48	51	1
Mar-26	14	0	61	65	1
Mar-27	5	0	66	70	1
Mar-28	27	0	93	97	1
Mar-29	14	0	107	111	1
Mar-30	20	1	121	131	2
Mar-31	4	0	125	135	2

Source: https://www.kaggle.com

As shown in the figure, COVID-19 total and active cases in Nigeria started to escalate from April 18th, 2020.

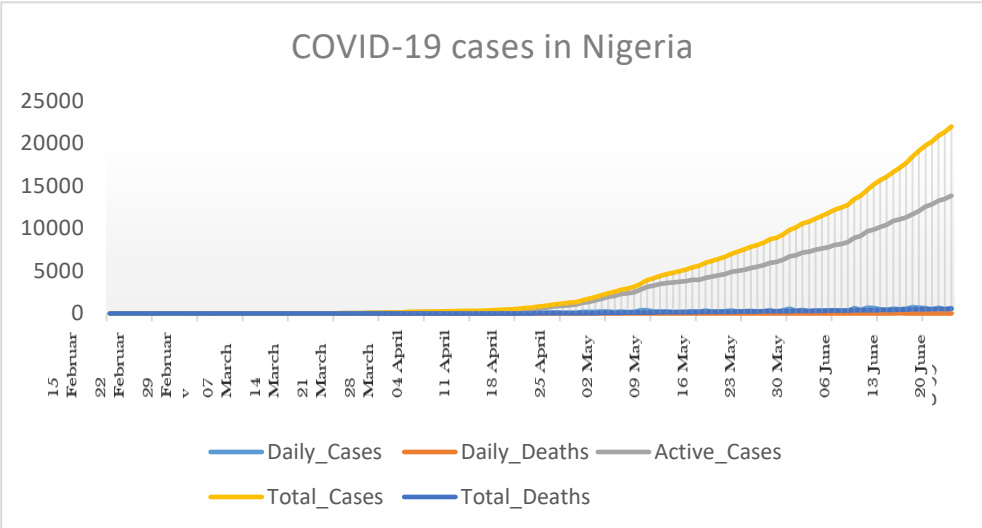

Fig. 4. Chart showing the trend of COVID-19 cases in Nigeria from June 15th to 24th, 2020.

4 | Performance Evaluation

The metrics employed to evaluate the performance of the models are the root mean squared error (RMSE), Mean Absolute Error (MAE) and Mean Absolute Percentage Error (MAPE).

$$\mathrm{RMSE} = \sqrt{\frac{1}{T}\sum_{t=1}^{T}\left(y^{a} - y\right)^{2}}. \tag{27}$$

$$\mathrm{MAE} = \frac{1}{T}\sum_{t=1}^{T}\left|y^{a} - y\right|. \tag{28}$$

$$\mathrm{MAPE} = \frac{1}{T}\sum_{t=1}^{T}\frac{\left|y^{a} - y\right|}{y^{a}} * 100. \tag{29}$$

Where y^{a} is the real output and y is the predicted output of the different prediction models.

Shown in *Fig. 5* to *Fig. 9* are the prediction performances of IFLS and FLS. As shown in most of the figures, the predicted outputs of IFLS tend to follow the actual outputs as closely as possible compared to the classical FLS. In particular, *Fig. 7* shows the classical FLS performing poorly in the prediction of the active COVID-19 pandemic cases. This is an indication that the classical FLS may not be a very robust model that can provide more accurate estimates in the face of uncertainty in most cases. However, a closer look at *Fig. 5* shows that the traditional FLS aligns closely with the actual values more than the IFLS. This is also revealed in *Table 2* with FLS yielding lower absolute average prediction error than IFLS. Shown in *Fig. 10* is a single instance of the adaptation of the user defined parameter, β, of IFLS.

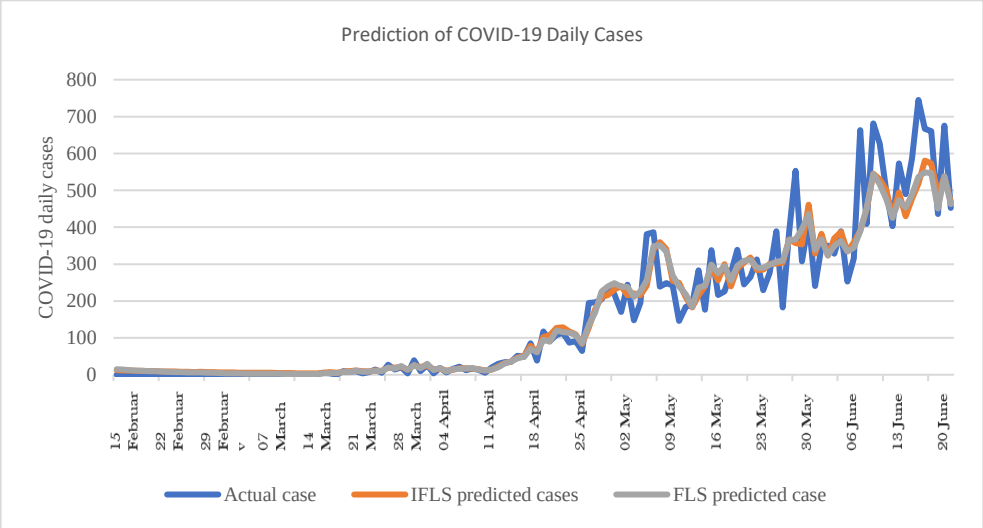

Fig. 5. Comparison of actual and predicted daily cases of COVID-19 in Nigeria using IFLS and FLS.

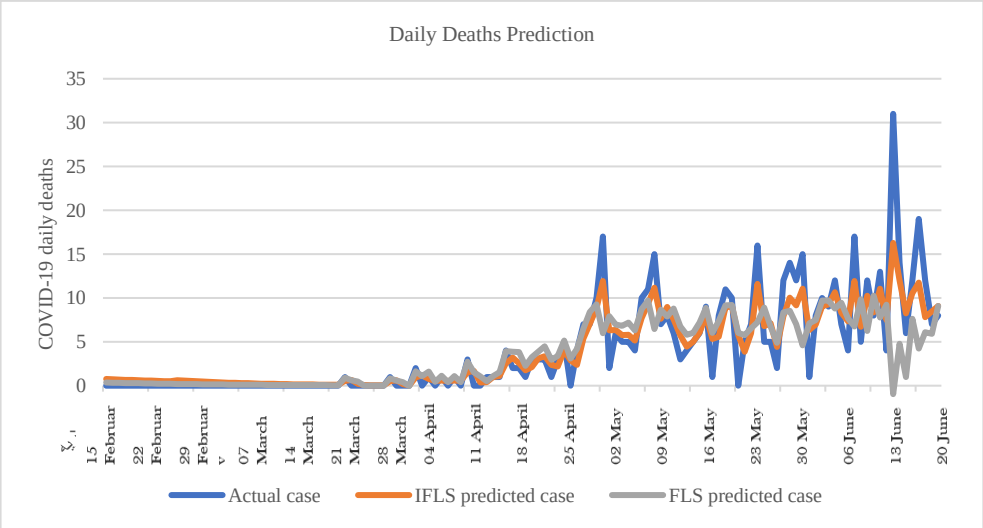

Fig. 6. Actual and predicted daily deaths from COVID-19.

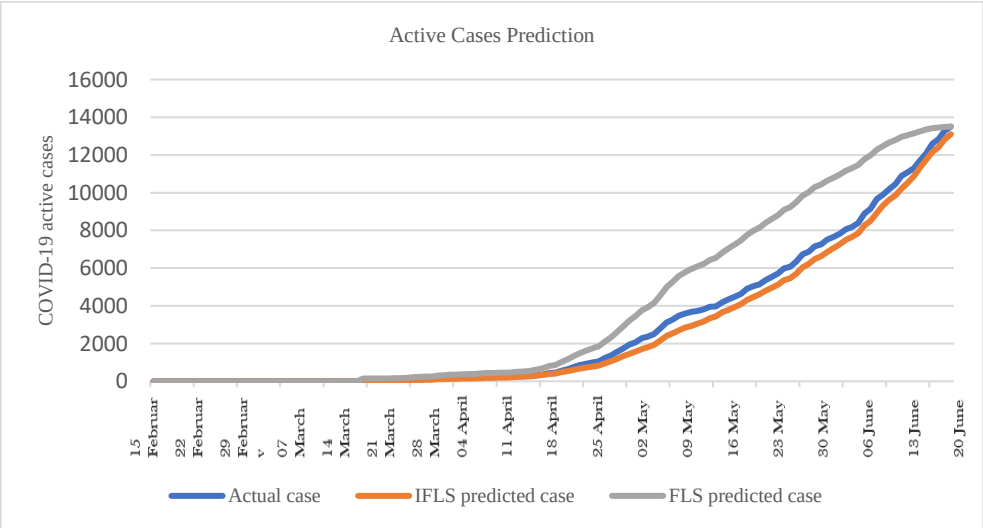

Fig. 7. Actual and predicted active cases of COVID-19.

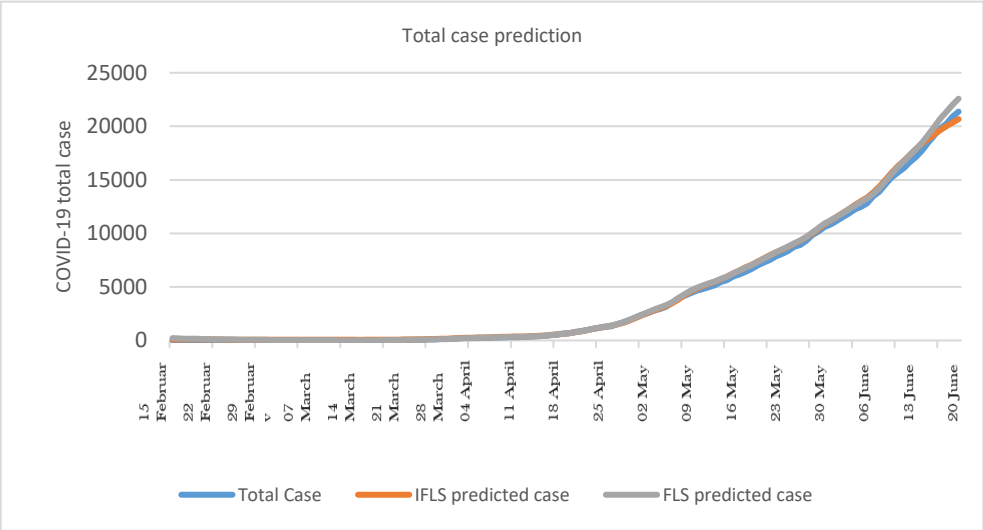

Fig. 8. Graph showing actual and predicted outputs of COVID-19 total cases.

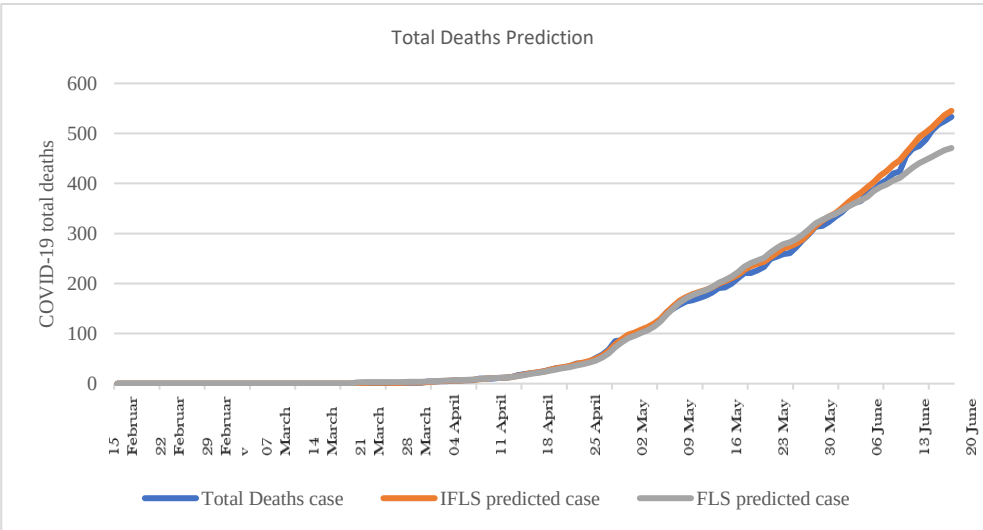

Fig. 9. Graph showing actual and predicted values of total deaths from COVID-19.

Tables 2-8 show the comparison of the actual and predicted numbers of the different cases of COVID-19 pandemic in Nigeria using classical FLS and IFLS with their corresponding absolute prediction errors. Interestingly, IFLS performs better overall as shown in the actual and predicted number of cases and the lower average absolute prediction errors (see *Tables 3-6*).

Table 2. Comparison of actual and predicted COVID-19 daily cases using IFLS and traditional type-1 FLS.

Day	Actual case	IFLS predicted case	FLS predicted case	IFLS predicted error	FLS predicted error
14-Jun	403	431.7257	425.6794	28.7257	22.6794
15-Jun	573	493.8253	473.382	79.1747	99.618
16-Jun	490	429.6738	453.1943	60.3262	36.8057
17-Jun	587	477.6494	489.0567	109.3506	97.9433
18-Jun	745	518.0091	536.6998	226.9909	208.3002
19-Jun	667	580.5806	548.7646	86.4194	118.2354
20-Jun	661	572.9636	546.8389	88.0364	114.1611
21-Jun	436	488.4975	450.5051	52.4975	14.5051
22-Jun	675	537.1518	538.3174	137.8482	136.6826
23-Jun	452	468.4112	462.9581	16.4112	10.9581
	Average error			88.57808	85.98889

Table 3. Comparison of actual and predicted COVID-19 daily deaths using IFLS and traditional Type-1 FLS.

Day	Actual case	IFLS predicted case	FLS predicted case	IFLS predicted error	FLS predicted error
14-Jun	13	11.0428	7.78	1.9572	5.22
15-Jun	4	7.4865	9.2303	3.4865	5.2303
16-Jun	31	16.2782	-0.9636	14.7218	31.9636
17-Jun	14	11.9934	4.7803	2.0066	9.2197
18-Jun	6	8.2303	0.9676	2.2303	5.0324
19-Jun	12	10.5317	7.637	1.4683	4.363
20-Jun	19	11.7382	4.243	7.2618	14.757
21-Jun	12	7.814	6.0818	4.186	5.9182
22-Jun	7	8.4769	5.9029	1.4769	1.0971
23-Jun	8	9.1006	9.0768	1.1006	1.0768
	Average error			3.9896	8.38781

Table 4. Comparison of actual and predicted COVID-19 active cases using IFLS and traditional Type-1 FLS.

Day	Actual case	IFLS predicted case	FLS predicted case	IFLS predicted error	FLS predicted error
14-Jun	10445	9861.75	12792.46	583.25	2347.462
15-Jun	10885	10212.75	12955.82	672.25	2070.819
16-Jun	11070	10512.45	13049.24	557.55	1979.235
17-Jun	11299	10872.9	13145.2	426.1	1846.199
18-Jun	11698	11329.2	13256.55	368.8	1558.55
19-Jun	12079	11738.25	13346.67	340.75	1267.674
20-Jun	12584	12143.25	13425.99	440.75	841.9872
21-Jun	12847	12410.55	13461.73	436.45	614.7342
22-Jun	13285	12825	13492.13	460	207.131
23-Jun	13500	13101.75	13500	398.25	0
	Average error			468.415	1273.379

Table 5. Comparison of Actual and Predicted COVID-19 Total Cases using IFLS and Traditional Type-1 FLS.

Day	Actual case	IFLS predicted case	FLS predicted case	IFLS predicted error	FLS predicted error
14-Jun	16085	16785	16761	700	676
15-Jun	16658	17339	17319	681	661
16-Jun	17148	17894	17872	746	724
17-Jun	17735	18395	18491	660	756
18-Jun	18480	18807	19189	327	709
19-Jun	19147	19231	19943	84	796
20-Jun	19808	19641	20715	167	907
21-Jun	20244	20009	21362	235	1118
22-Jun	20919	20349	22009	570	1090
23-Jun	21371	20671	22575	700	1204
	Average error			487	864.1

Table 6. Comparison of actual and predicted COVID-19 total deaths using IFLS and traditional Type-1 FLS.

Day	Actual case	IFLS predicted case	FLS predicted case	IFLS predicted error	FLS predicted error
14-Jun	420	437.2488	405.9877	17.2488	14.0123
15-Jun	424	446.2144	411.2714	22.2144	12.7286
16-Jun	455	461.3492	421.4614	6.3492	33.5386
17-Jun	469	476.0808	431.2186	7.0808	37.7814
18-Jun	475	492.2251	440.7627	17.2251	34.2373
19-Jun	487	501.7825	446.6526	14.7825	40.3474
20-Jun	506	512.3679	453.2103	6.3679	52.7897
21-Jun	518	525.1286	460.3934	7.1286	57.6066
22-Jun	525	536.7947	466.5433	11.7947	58.4567
23-Jun	533	545.0093	470.7669	12.0093	62.2331
	Average error			12.22013	40.37317

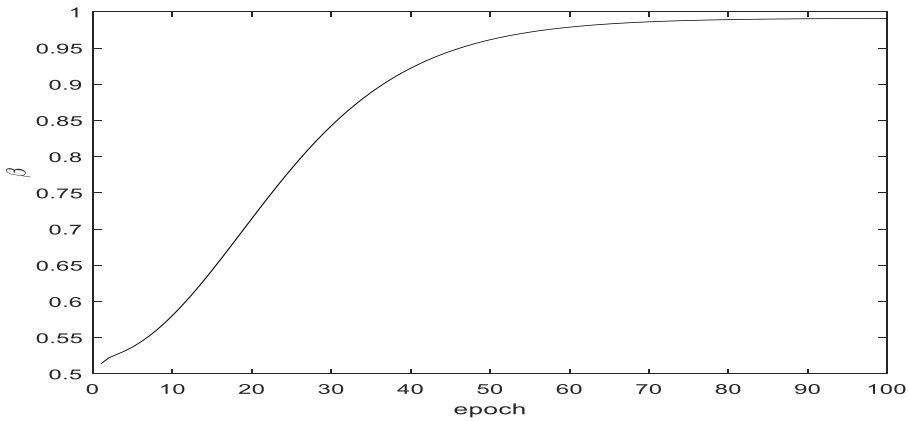

Fig. 10. A scenario showing the adaptation of the user defined parameter, β, of IFLS.

For further comparison, an experiment is conducted to compare the performances of the FLS approaches with ANN, where ANN forms an integral part of these FLSs. The GD-backpropagation is used to learn the parameters of the ANN. However, the number of hidden neurons for the ANN is set to 5 as it provided the smallest errors. Every other computational set-up is the same as those for the FLSs. Shown in *Table 7* are the errors for the different models and for the different cases of COVID-19 in Nigeria. As shown in the table, IFLS with MFs and NMFs together with the hesitation indices exhibits more acceptable performance in terms of RMSE, MAE and MAPE with reduced average absolute errors compared to traditional FLS with only MFs. The IFLS also outperforms the standalone

ANN. The integration of ANN in the FLSs (IFLS and FLS), however, provided a synergistic capability for effective handling of uncertainty than the standalone ANN. In the overall, the FLSs provided better performances than the ANN. The plot of the variations in the RMSE of the different models for different COVID-19 cases are shown in *Fig. 11*. The lower the RMSE, the better the performance.

Table 7. Performance of FLS, IFLS and ANN on cases of COVID-19 based on different performance metrics.

COVID-19 cases	Metrics	FLS	ANN	IFLS
Daily cases	RMSE	106.4437	233.5901	104.6956
	MAE	87.3931	193.9882	87.4217
	MAPE (%)	17.038	32.5901	16.1937
Daily deaths	RMSE	7.4546	7.8208	6.7965
	MAE	4.9938	5.338	4.4439
	MAPE (%)	41.4715	45.6242	43.1968
Active cases	RMSE	1718.404	2870.6	1530.1769
	MAE	1481.424	2614.1	1286.7551
	MAPE (%)	13.4793	21.051	11.3811
Total cases	RMSE	1598.213	2063.1	1505.5709
	MAE	1313.287	1811.5	1254.4038
	MAPE (%)	8.2875	9.8775	7.3991
Total deaths	RMSE	67.192	178.8472	57.4778
	MAE	60.2266	173.0478	45.3706
	MAPE (%)	13.5011	35.4769	10.4515

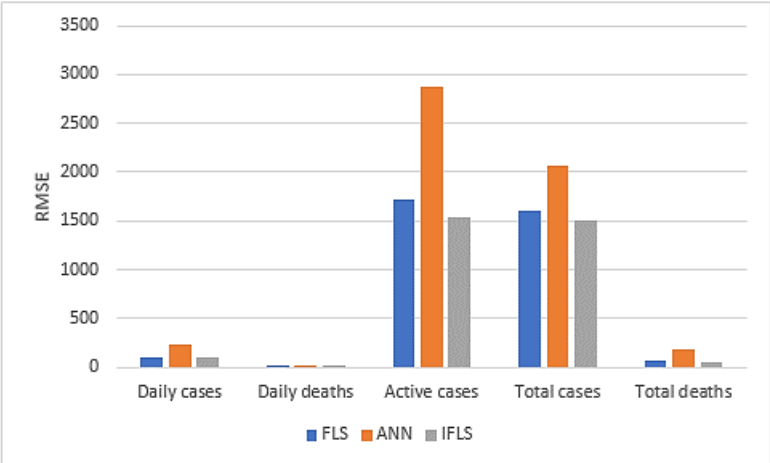

Fig. 11. RMSE for each model and COVID-19 case.

Analysis is also conducted to compare the average running times of the various models in the prediction of COVID-19 cases as depicted in *Table 8*.

Table 8. Comparison of running time of FLS, IFLS and ANN.

Model	Average running time (sec)
FLS	4.38
IFLS	10.33
ANN	13.28

As shown in *Table 8*, classical fuzzy logic system exhibits the lowest computational time compared to IFLS and ANN. This implies that if running time is of essence, then traditional FLS may be a good choice in these problem cases.

5 | Conclusion

In this study, IFLS was applied to analyze the prediction capability using COVID-19 data in Nigeria, the second most affected country with COVID-19 in Africa. To aid comparison, classical type-1 FLS and traditional neural networks were also employed. As shown in the tables, IFLS with MFs and NMFs outperforms the two competing models (FLS and ANN) in four of the COVID-19 cases based on the error metrics with decreasing errors. The presence of NMFs and hesitation indices provides more design degrees of freedom and flexibility for IFLS to handle uncertainty and vagueness well. Moreover, IFLS is an adaptive system, allowing the system to cope with the changing nature of COVI-19 pandemic. Optimizing the parameters of the IFLS helps to enhance prediction and generalization capability of the model. IFLS can therefore stand as a robust model for the prediction of COVID-19 pandemic cases. IFLS however incurs more computational cost than the classical FLS and may not be applicable in situation where running time is paramount. Overall, the FLS models outperform the single neural network model both in terms of accuracy and running time. However, IFLS has MF and NMFs that are precise and may not handle uncertainty well in many situations. Hence, in the future, we intend to use higher order fuzzy logic systems such as classical type-2 FLS with fuzzy MFs and type-2 intuitionistic FLS with fuzzy MFs and NMFs for the analysis of the COVID-19 pandemic cases. These higher order FLSs are expected to efficiently handle uncertainties and minimize their effects on the predicted COVID-19 pandemic cases. A study will also be conducted to include other African countries mostly affected by the COVID-19 pandemic.

References

[1] World Health Organization, Coronavirus disease (COVID-19) outbreak. Retrieved July 1, 2020, from https://www.who.int/emergencies/diseases/novel-coronavirus-2019

[2] Patra, G. R., Das, A., & Mohanty, M. N. (2020). A time-series prediction model using long-short term memory networks for prediction of Covid – 19 data. *International journal of advanced science and technology*, *29*(12), 2179-2183.

[3] Pandey, G., Chaudhary, P., Gupta, R., & Pal, S. (2020). SEIR and regression model based COVID-19 outbreak predictions in India. arXiv preprint arXiv:2004.00958.

[4] Melin, P., Monica, J. C., Sanchez, D., & Castillo, O. (2020, June). Multiple ensemble neural network models with fuzzy response aggregation for predicting COVID-19 time series: the case of Mexico. In *healthcare*, *8*(2), 181, multidisciplinary digital publishing institute. https://doi.org/10.3390/healthcare8020181

[5] Bastos, S. B., & Cajueiro, D. O. (2020). Modeling and forecasting the early evolution of the Covid-19 pandemic in Brazil. *Scientific reports*, *10*(1), 1-10. https://doi.org/10.1038/s41598-020-76257-1

[6] Zhao, S., & Chen, H. (2020). Modeling the epidemic dynamics and control of COVID-19 outbreak in China. *Quantitative biology*, *8*, 11-19. https://doi.org/10.1007/s40484-020-0199-0

[7] Roosa, K., Lee, Y., Luo, R., Kirpich, A., Rothenberg, R., Hyman, J. M., Yan, P., & Chowell, G. B. (2020). Real-time forecasts of the COVID-19 epidemic in China from February 5th to February 24th, 2020. *Infectious disease modelling*, *5*, 256-263. https://doi.org/10.1016/j.idm.2020.02.002

[8] Anastassopoulou, C., Russo, L., Tsakris, A., & Siettos, C. (2020). Data-based analysis, modelling and forecasting of the COVID-19 outbreak. *PloS one*, *15*(3), e0230405. https://doi.org/10.1371/journal.pone.0230405

[9] Chimmula, V. K. R., & Zhang, L. (2020). Time series forecasting of COVID-19 transmission in Canada using LSTM networks. *Chaos, Solitons & Fractals*, *135*, 109864. https://doi.org/10.1016/j.chaos.2020.109864

[10] Alboaneen, D., Pranggono, B., Alshammari, D., Alqahtani, N., & Alyaffer, R. (2020). Predicting the epidemiological outbreak of the coronavirus disease 2019 (COVID-19) in Saudi Arabia. *International journal of environmental research and public health*, *17*(12), 4568. https://doi.org/10.3390/ijerph17124568

[11] Ceylan, Z. (2020). Estimation of COVID-19 prevalence in Italy, Spain, and France. *Science of the total environment*, *729*, 138817. https://doi.org/10.1016/j.scitotenv.2020.138817

[12] Ribeiro, M. H. D. M., da Silva, R. G., Mariani, V. C., & dos Santos Coelho, L. (2020). Short-term forecasting COVID-19 cumulative confirmed cases: Perspectives for Brazil. *Chaos, solitons and fractals*, *135*, 109853. https://doi.org/10.1016/j.chaos.2020.109853

[13] Pinter, G., Felde, I., Mosavi, A., Ghamisi, P., & Gloaguen, R. (2020). COVID-19 pandemic prediction for Hungary; a hybrid machine learning approach. *Mathematics*, *8*(6), 890. https://doi.org/10.3390/math8060890

[14] Remuzzi, A., & Remuzzi, G. (2020). COVID-19 and Italy: what next?. *The lancet*, *395*(10231), 1225-1228. https://doi.org/10.1016/S0140-6736(20)30627-9

[15] Rovetta, A., Bhagavathula, A. S., & Castaldo, L. (2020). Modeling the epidemiological trend and behavior of COVID-19 in Italy. *Cureus*, *12*(8), e9884. DOI: 10.7759/cureus.9884

[16] Alsayed, A., Sadir, H., Kamil, R., & Sari, H. (2020). Prediction of epidemic peak and infected cases for COVID-19 disease in Malaysia, 2020. *International journal of environmental research and public health*, *17*(11), 4076. https://doi.org/10.3390/ijerph17114076

[17] Kuniya, T. (2020). Prediction of the epidemic peak of coronavirus disease in Japan, 2020. *Journal of clinical medicine*, *9*(3), 789. https://doi.org/10.3390/jcm9030789

[18] Olfatifar, M., Houri, H., Shojaee, S., Pourhoseingholi, M. A., Alali, W. Q., Busani, L., ... & Asadzadeh Aghdaei, H. (2020). The required confronting approaches efficacy and time to control COVID-19 outbreak in Iran. *Archives of clinical infectious diseases*, *15*(COVID-19). DOI: 10.5812/archcid.102633

[19] Petropoulos, F., & Makridakis, S. (2020). Forecasting the novel coronavirus COVID-19. *PloS one*, *15*(3), e0231236. https://doi.org/10.1371/journal.pone.0231236

[20] Eyoh, I., John, R., & De Maere, G. (2017, July). Time series forecasting with interval type-2 intuitionistic fuzzy logic systems. *2017 IEEE international conference on fuzzy systems (FUZZ-IEEE)* (pp. 1-6). IEEE. DOI: 10.1109/FUZZ-IEEE.2017.8015463

[21] Al-Qaness, M. A., Ewees, A. A., Fan, H., & Abd El Aziz, M. (2020). Optimization method for forecasting confirmed cases of COVID-19 in China. *Journal of clinical medicine*, *9*(3), 674. https://doi.org/10.3390/jcm9030674

[22] Dhiman, N., & Sharma, M. (2020). Fuzzy logic inference system for identification and prevention of Coronavirus (COVID-19). *International journal of innovative technology and exploring engineering*, *9*(6).

[23] Fong, S. J., Li, G., Dey, N., Crespo, R. G., & Herrera-Viedma, E. (2020). Composite Monte Carlo decision making under high uncertainty of novel coronavirus epidemic using hybridized deep learning and fuzzy rule induction. *Applied soft computing*, *93*, 106282. https://doi.org/10.1016/j.asoc.2020.106282

[24] Fatima, S. A., Hussain, N., Balouch, A., Rustam, I., Saleem, M., & Asif, M. (2020). IoT enabled smart monitoring of coronavirus empowered with fuzzy inference system. *International journal of advance research, ideas and innovations in technology*, *6*(1), 188-194.

[25] Verma, P., Khetan, M., Dwivedi, S., & Dixit, S. (2020). Forecasting the covid-19 outbreak: an application of arima and fuzzy time series models. DOI: 10.21203/rs.3.rs-36585/v1

[26] Van Tinh, N. (2020). Forecasting of COVID-19 Confirmed cases in Vietnam using fuzzy time series model combined with particle swarm optimization. *Comput. Res. Progr. Appl. Sci. Eng.*, *6*(2), 114-120.

[27] Kumar, M. (2019). Evaluation of the intuitionistic fuzzy importance of attributes based on the correlation coefficient under weakest triangular norm and application to the hotel services. *Journal of intelligent & fuzzy systems*, *36*(4), 3211-3223. DOI: 10.3233/JIFS-18485

[28] Atanassov, K. T. (1999). Intuitionistic fuzzy sets. In *Intuitionistic fuzzy sets* (pp. 1-137). Physica, Heidelberg.

[29] Wang, Y. N., Lei, Y., Fan, X., & Wang, Y. (2016). Intuitionistic fuzzy time series forecasting model based on intuitionistic fuzzy reasoning. *Mathematical problems in engineering*. https://doi.org/10.1155/2016/5035160

[30] Bisht, K., Joshi, D. K., & Kumar, S. (2018). Dual hesitant fuzzy set-based intuitionistic fuzzy time series forecasting. In *Ambient communications and computer systems* (pp. 317-329). Singapore: Springer. https://doi.org/10.1007/978-981-10-7386-1_28

[31] Bas, E., Yolcu, U., & Egrioglu, E. (2020). Intuitionistic fuzzy time series functions approach for time series forecasting. *Granular computing*, 1-11.

[32] Abhishekh, Gautam, S. S., & Singh, S. R. (2020). A new method of time series forecasting using intuitionistic fuzzy set based on average-length. *Journal of industrial and production engineering*, *37*(4), 175-185. https://doi.org/10.1080/21681015.2020.1768163

[33] Tak, N. (2020). Type-1 recurrent intuitionistic fuzzy functions for forecasting. *Expert systems with applications*, *140*, 112913. https://doi.org/10.1016/j.eswa.2019.112913

[34] Fan, X., Wang, Y., & Zhang, M. (2020). Network traffic forecasting model based on long-term intuitionistic fuzzy time series. *Information sciences*, *506*, 131-147. https://doi.org/10.1016/j.ins.2019.08.023

[35] Eyoh, I., John, R., De Maere, G., & Kayacan, E. (2018). Hybrid learning for interval type-2 intuitionistic fuzzy logic systems as applied to identification and prediction problems. *IEEE Transactions on fuzzy systems*, *26*(5), 2672-2685. DOI: 10.1109/TFUZZ.2018.2803751

[36] Imtiaz, M., Saqlain, M., & Saeed, M. (2020). TOPSIS for multi criteria decision making in octagonal intuitionistic fuzzy environment by using accuracy function. *Journal of new theory*, (31), 32-40.

[37] Castillo, O., Kutlu, F., & Atan, Ö. (2020). Intuitionistic fuzzy control of twin rotor multiple input multiple output systems. *Journal of intelligent and fuzzy systems*, *38*(1), 821-833. doi: 10.3233/JIFS-179451

[38] Kabir, S., Geok, T. K., Kumar, M., Yazdi, M., & Hossain, F. (2019). A method for temporal fault tree analysis using intuitionistic fuzzy set and expert elicitation. *IEEE access*, *8*, 980-996. DOI: 10.1109/ACCESS.2019.2961953

[39] Kumar, M., & Kaushik, M. (2020). System failure probability evaluation using fault tree analysis and expert opinions in intuitionistic fuzzy environment. *Journal of loss prevention in the process industries*, *67*, 104236. https://doi.org/10.1016/j.jlp.2020.104236

[40] Edalatpanah, S. A. (2019). A data envelopment analysis model with triangular intuitionistic fuzzy numbers. *International journal of data envelopment analysis*, *7*(4), 47-58.

[41] Ejegwa, P. A., & Onyeke, I. C. (2020). Medical diagnostic analysis on some selected patients based on modified Thao et al.'s correlation coefficient of intuitionistic fuzzy sets via an algorithmic approach. *Journal of fuzzy extension and applications*, *1*(2), 130-141.

[42] Khatibi, V., & Montazer, G. A. (2009). Intuitionistic fuzzy set vs. fuzzy set application in medical pattern recognition. *Artificial intelligence in medicine*, *47*(1), 43-52. https://doi.org/10.1016/j.artmed.2009.03.002

[43] Rahman, A. U., Ahmad, M. R., Saeed, M., Ahsan, M., Arshad, M., & Ihsan, M. (2020). A study on fundamentals of refined intuitionistic fuzzy set with some properties. *Journal of fuzzy extension and applications*, *1*(4), 300-314.

[44] Zadeth, L. A. (1965). Fuzzy sets. *Information and control*, *8*(3), 338-353.

[45] Radhika, C., & Parvathi, R. (2016). Intuitionistic fuzzification functions. *Global Journal of pure and applied mathematics*, *12*(2), 1211-1227.

[46] Hájek, P., & Olej, V. (2015, September). Intuitionistic fuzzy neural network: The case of credit scoring using text information. *International conference on engineering applications of neural networks* (pp. 337-346). Cham Springer. https://doi.org/10.1007/978-3-319-23983-5_31

[47] Mahapatra, G. S., & Roy, T. K. (2013). Intuitionistic fuzzy number and its arithmetic operation with application on system failure. *Journal of uncertain systems*, *7*(2), 92-107.

[48] Imo Jeremiah, E. Y. O. H. (2018). *Interval type-2 Atanassov-intuitionistic fuzzy logic for uncertainty modelling* (Doctoral dissertation, University of Nottingham), PhD thesis, University of Nottingham. Retrieved from http://eprints.nottingham.ac.uk/51441/

[49] Hájek, P., & Olej, V. (2014, August). Defuzzification methods in intuitionistic fuzzy inference systems of Takagi-Sugeno type: the case of corporate bankruptcy prediction. *11th international conference on fuzzy systems and knowledge discovery (FSKD)* (pp. 232-236). IEEE. DOI: 10.1109/FSKD.2014.6980838

[50] Africa COVID-19 Daily Cases. (2020). Retrieved June 27, 2020 from https://www.kaggle.com/mohammedessam97/africa-covid19-daily-cases

[51] Elmousalami, H. H., & Hassanien, A. E. (2020). Day level forecasting for Coronavirus Disease (COVID-19) spread: analysis, modeling and recommendations. arXiv preprint arXiv:2003.07778